POLYMERS

Recyclable surgical, consumer, and industrial adhesives of poly(α-lipoic acid)

Subhajit Pal[1], Jisoo Shin[1], Kelsey DeFrates[1], Mustafa Arslan[1,2], Katelyn Dale[1], Hannah Chen[3], Dominic Ramirez[1], Phillip B. Messersmith[1,3,4]*

Polymer adhesives play an important role in many medical, consumer, and industrial products. Polymers of α-lipoic acid (αLA) have the potential to fulfill the need for versatile and environmentally friendly adhesives, but their performance is plagued by spontaneous depolymerization. We report a family of stabilized αLA polymer adhesives that can be tailored for a variety of medical or nonmedical uses and sustainably sourced and recycled in a closed-loop manner. Minor changes in monomer composition afforded a pressure-sensitive adhesive that functions well in dry and wet conditions, as well as a structural adhesive with strength equivalent to that of conventional epoxies. αLA surgical superglue successfully sealed murine amniotic sac ruptures, increasing fetal survival from 0 to 100%.

Polymer adhesives play a crucial and sometimes hidden role in consumer, industrial, and medical products (*1*). A large variety of adhesive polymer compositions, physical properties, and form factors are in use today, reflecting the diverse performance requirements of major categories such as pressure-sensitive adhesives (PSAs), structural adhesives, and medical adhesives. A long-standing paradigm in polymer adhesives is that excellent performance in one context does not typically translate to other contexts. As a result, the compositions and physical properties of most commercially available polymer adhesives are tailored for specific, sometimes narrow uses. There is a need for multipurpose polymer adhesives that perform well across a range of surface compositions, roughness, and environmental conditions (*2*–*5*). Moreover, there is a growing awareness of the need to address the environmental impact of polymer adhesives (*6*). Although efforts are underway to derive adhesives from renewable resources (*7*–*11*), most existing PSAs and structural adhesives are derived from nonrenewable resources and are used once before ending up in the environment, landfill, or incinerator. A desirable polymer adhesive platform would be effective in a broad range of practical settings, manufactured from sustainable or natural feedstocks, and amenable to closed-loop recycling of monomer and polymer.

(R)-α-lipoic acid (αLA, Fig. 1A) is an essential cofactor for enzymes involved in aerobic metabolism. αLA has been reported to undergo thermal (*12*–*16*), ionic (*17*–*21*), and controlled radical ring-opening polymerization (*22*). Polymers of αLA could be useful in a variety of practical settings and are amenable to closed-loop recycling (*12*–*14*, *19*, *22*), but they suffer from spontaneous depolymerization under conditions relevant to many real-world applications (*12*, *14*, *15*). Focusing on the potential role of the active chain end radical in depolymerization (*12*, *13*, *16*), multiple attempts have been made to stabilize poly(α-lipoic acid) by exploiting the radical-quenching properties of comonomers, polyphenols, and other species (*12*, *13*, *22*–*24*). We report a facile method for catalyst-free αLA polymerization, affording polymers that are resistant to spontaneous depolymerization. A small library of αLA monomer derivatives provided access to a surprisingly wide range of physical properties and uses.

Rapid polymerization and chain end stabilization of αLA polymers by chemical modification of αLA monomers

We focused on influencing αLA polymerization and depolymerization through manipulation of monomer chemical composition, with the goal of rapid solution polymerization of a water-stable polymer at ambient temperature. Consistent with an early report that showed rapid oligomerization of conformationally strained cyclic disulfides in the solution state at physiological conditions (*25*), we observed that the addition of excess phosphate-buffered saline (PBS) to a concentrated ethanolic solution of αLA resulted in immediate formation of an intractable sticky polymer (fig. S1) that rapidly (<5 min) underwent depolymerization to yield insoluble monomeric solids. We therefore concluded that controlling the depolymerization of αLA polymers, especially in wet environments, represents a key to the practical use of αLA polymers.

We hypothesized that the metastable (polymeric) state could be stabilized through the addition of an electrophile that prevents closed-loop depolymerization during storage and use (Fig. 1B and fig. S2). To test this hypothesis, we designed two *N*-hydroxy succinimide (NHS) esters of α-lipoic acid (S1 and S2, Fig. 1A) in view of the high stability of NHS-ester in alcoholic solvents and the accelerating effect of activated ester (NHS) on cationic polymerization (*26*). An ethanolic solution of αLA and S1 or S2 was prepared at a mole ratio of 93:7, and a small amount of dimethyl sulfoxide (DMSO) was added to ensure the solubility of the NHS esters (see materials and methods). Detailed ^{1}H nuclear magnetic resonance (NMR) experiments of diluted ethanolic solution of the mixtures showed excellent stability of the NHS esters over an extended period (figs. S3 and S4). To confirm the participation of activated ester in the polymerization, we prepared 400 mg/ml ethanolic solutions of αLA and S1 or S2 mixtures and monitored them over time. The concentrated ethanolic solution of αLA alone did not form a gel within 2 days, suggesting that the monomer-polymer equilibrium strongly favors the monomeric state (Fig. 1B and fig. S5). However, the ethanolic mixture of αLA with S2 or S1 at a similar concentration formed a gel within 30 min or 1 hour, respectively, and showed an inverse correlation of gelation time with monomer concentration (Fig. 1C and figs. S5 and S6). These results established the efficacy of NHS

Table 1. Adhesive systems based on stabilized αLA polymers.

Adhesive	Purpose	Form*	Composition (mol %)				
			αLA	S1	S2	NaLA	CaLA
αLA-MS1	Medical superglue (spray)	L	93	7	–	–	–
αLA-MS2	Medical superglue (spray)	L	93	–	7	–	–
αLA-MS3	Medical superglue (brush)	L	70	7	–	23	–
αLA-MS4	Medical superglue (patch)	S	93	7	–	–	–
αLA-MS5	Medical superglue (patch)	S	93	–	7	–	–
αLA-PSA	Pressure-sensitive adhesive	S	93	–	7	–	–
αLA-SA	Structural adhesive	S,P	75	6	–	–	19

*L, liquid; S, solid patch or film; P, powder.

[1]Department of Bioengineering, University of California, Berkeley, CA 94720, USA. [2]Department of Chemistry, Faculty of Science and Letters, Kirklareli University, Kirklareli 39100, Türkiye. [3]Department of Materials Science and Engineering, University of California, Berkeley, CA 94720, USA. [4]Materials Sciences Division, Lawrence Berkeley National Laboratory, Berkeley, CA 94720, USA.
*Corresponding author. Email: philm@berkeley.edu

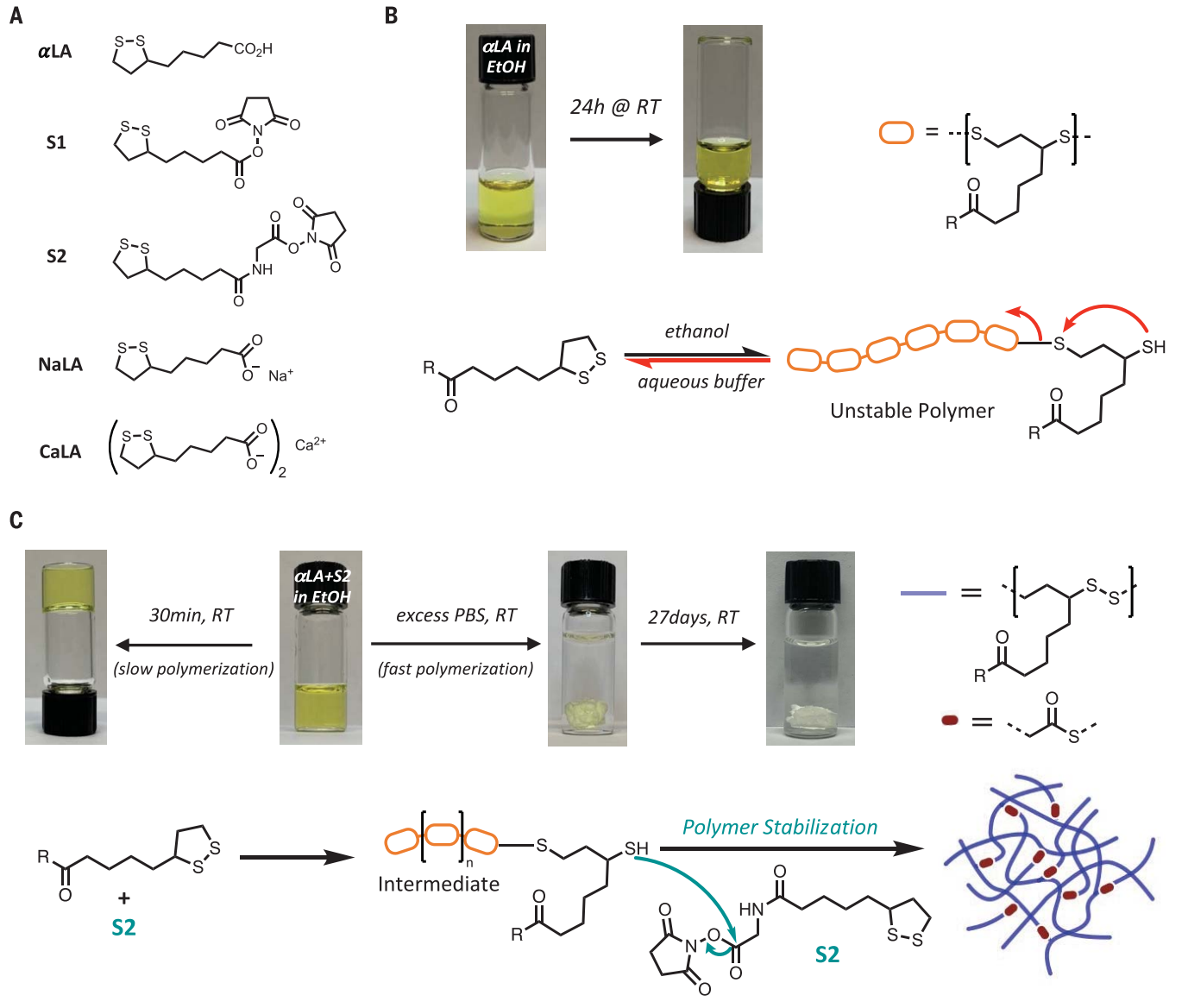

Fig. 1. Monomer structures and general scheme of polymerization from precursor solution. (**A**) Chemical structure of monomers. (**B**) Photographs of ethanolic αLA solution taken initially (left) and after 24 hours at room temperature (right) indicate that pure αLA does not polymerize in ethanol. Addition of aqueous buffer induces polymerization; however, depolymerization to the monomer is rapid (fig. S1). A plausible mechanism for the aqueous depolymerization pathway is represented by the red arrows (below). (**C**) Photographs above left show the spontaneous copolymerization of ethanolic solutions of αLA and stabilizer S2 within 30 min, illustrating the stabilizing effect of S2. Notably, addition of excess aqueous buffer to a fresh ethanolic solution of αLA and stabilizer S2 resulted in immediate formation of a stable polymer (photographs above right). A generalized scheme of polymerization and polymer chain end stabilization is shown below. In the reaction schemes, R varies by solvent and pH: R is OH in ethanol, whereas R is O^- in buffered aqueous solvent at pH values above the pK_a (acid dissociation constant) of the carboxylic acid (~4.5).

esters in both stabilizing the chain end and promoting the polymerization of αLA. The faster gelation time with S2 compared to S1 was attributed to the higher electrophilicity of S2. Moreover, the chain end stabilization of αLA polymerization is not only limited to NHS esters; other activated electrophilic functional groups such as isocyanate, anhydride, oxidized polyphenol, etc., were able to stabilize the αLA polymer (fig. S6).

When an ethanolic solution of αLA and S1 or S2 was added to water, we observed rapid polymerization, producing a stable elastomeric adhesive polymer (Fig. 1C, fig. S1, and movie S1) with a glass transition temperature (T_g) at −29°C (fig. S7). In the presence of S1 or S2, we speculate that αLA undergoes self-catalyzed cationic-like polymerization (*20*) followed by reaction of a chain end thiol with the NHS ester of S1/S2, yielding a thioester linkage and a terminal cyclic dithiolane group (Fig. 1C and fig. S2). Subsequent cascade branch polymerization (fig. S2) produces a polymer whose stability is further enhanced owing to the branched architecture. Polymerization of an ethanolic solution of αLA triggered by exposure to water appears to be extremely fast and largely insensitive to monomer concentration. Evidence for nanoparticle formation upon contact of αLA with water (fig. S1) led us to speculate that the amphiphilic nature of αLA drives self-aggregation, which locally concentrates the cyclic dithiolane to accelerate polymerization (*20*). Using this general approach, tailoring monomer composition (αLA:S1/S2 ratio plus the addition of NaLA or CaLA) gave rise

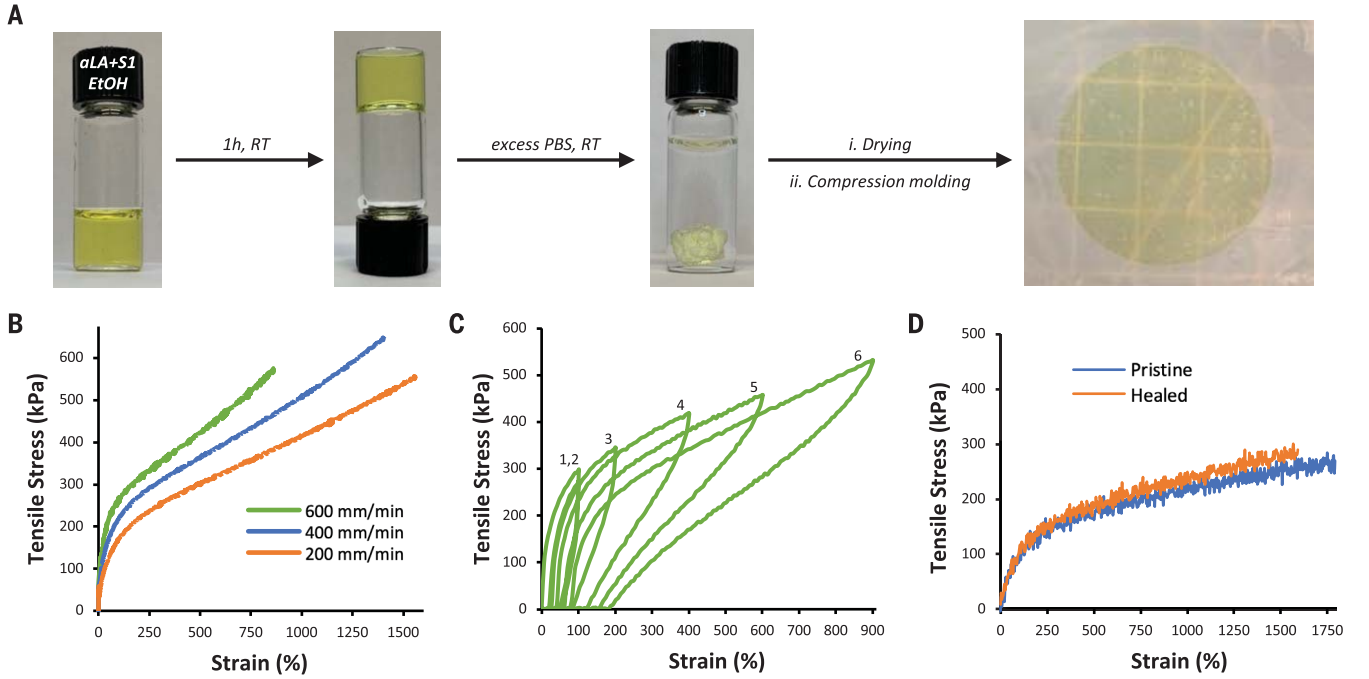

Fig. 2. Bulk mechanical properties of S1-stabilized αLA polymer. (**A**) αLA-MS4, formed by spontaneous polymerization of an ethanolic precursor mixture of αLA and S1 followed by precipitation in excess water, was dried and compression molded into a thin film for mechanical analysis. (**B**) Stress-strain curves of αLA-MS4 at different strain rates (rupture was observed at maximum strain) (N = 5). (**C**) Cyclic load-deformation curves of αLA-MS4 at a strain rate of 200 mm/min, measured with incremental increase in strain and no delay between cycles. Labels on each curve indicate the maximum percentage strain in each of six cycles: 1, 100; 2, 100; 3, 200; 4, 400; 5, 600; 6, 900 (N = 3). (**D**) Representative stress-strain curves of αLA-MS4 obtained at a strain rate of 200 mm/min for the pristine and ruptured polymer after 10 min of healing at 60°C. The pristine (unruptured) samples were treated at the same healing conditions for comparison. Average strain at rupture for the pristine and healed samples were 1644 ± 282% (N = 4) and 1568 ± 41 (N = 3), respectively. P = 0.6. P value was calculated with Student's t test in Microsoft Excel (2 array, 2 tails, 2 type). N is the number of independent repetitions.

to a family of versatile adhesives for medical, pressure-sensitive, and structural adhesive applications (Table 1).

To assess the bulk mechanical properties of stabilized αLA polymer, we prepared homogeneous thin films of αLA-MS4 by compression molding of the polymer obtained from aqueous polymerization of the precursor solution (Fig. 2A) (materials and methods). Stress-strain measurements show that the polymer could be stretched more than 10 times its initial length (1000% strain deformation) without rupture (Fig. 2B). A tensile modulus of 481 ± 60 kPa was calculated from the lower region of the stress-strain curve obtained at 200 mm/min. The viscoelastic nature of the polymer is apparent from the strain rate dependence of tensile modulus and strain to failure (Fig. 2B), hysteresis in cyclic load-deformation measurements (Fig. 2C and fig. S8), stress relaxation (fig. S8), creep (fig. S8), and dynamic rheology (fig. S9) measurements. Rheological data revealed the maturation of the high strain amplitude stiffness of the polymer over time (fig. S9), leading us to conclude that further polymerization and branching occurred (fig. S2) during the first 24 hours. Polymers of αLA are known to exhibit self-healing due to the presence of dynamic covalent disulfide bonds (*12*, *13*). To test this, we cut a polymer film into two pieces and then carefully brought the pieces into contact along the cut edges for 10 min at 60°C followed by equilibration for 10 min at room temperature. More than 95% of the original tensile strength was achieved in the healed sample (Fig. 2D and fig. S42), indicating fast dynamic exchange within the polymer network.

Stabilized αLA polymer as a surgical superglue

Of particular interest to us was to develop a rapid-setting, high-strength, biocompatible and biodegradable surgical tissue adhesive (*2*, *27*–*29*). Among approved medical adhesives, the gold standard in terms of mechanical performance is arguably cyanoacrylate superglue, a viscous liquid monomer that solidifies by polymerization within seconds of contact with tissue (*30*). Despite widespread use for external wound closure, medical cyanoacrylates are not widely approved for internal surgical use owing to concerns related to high stiffness, cytotoxicity, and slow degradation (*31*, *32*). Tissue adhesives based on thermal copolymerization of lipoic acid have been investigated for external wound closure (*23*, *24*, *33*–*35*); however, their slow curing time and several-fold-lower adhesion strength compared to medical cyanoacrylates preclude their use in mechanically demanding surgical settings. We developed several liquid and solid adhesive formulations that could be implemented by spraying, brushing, or pressing onto various tissues, producing an elastomeric polymer that bonds soft tissues together.

Spray, brush, and patch formulations of αLA superglue

Low-viscosity ethanolic precursor solutions of αLA and S1 or S2 (αLA-MS1 and αLA-MS2, Table 1) could be easily sprayed onto damp surfaces, resulting in rapid evaporation of the ethanol solvent and immediate in situ polymerization to generate a conformal polymer film on the wet substrate. Guided by current understanding of the polymerization mechanism of αLA derivatives (*20*), we also prepared a solvent-free viscous liquid that can be brushed or dropped onto wet tissue surfaces (αLA-MS3, Table 1; see materials and methods). The stabilized liquid underwent ultrafast polymerization when brought into contact with water (movie S2) to yield an adhesive polymer. A third variation took the form of a solid elastomeric patch (αLA-MS4 and αLA-MS5, Table 1) derived as described in Fig. 2 from solution

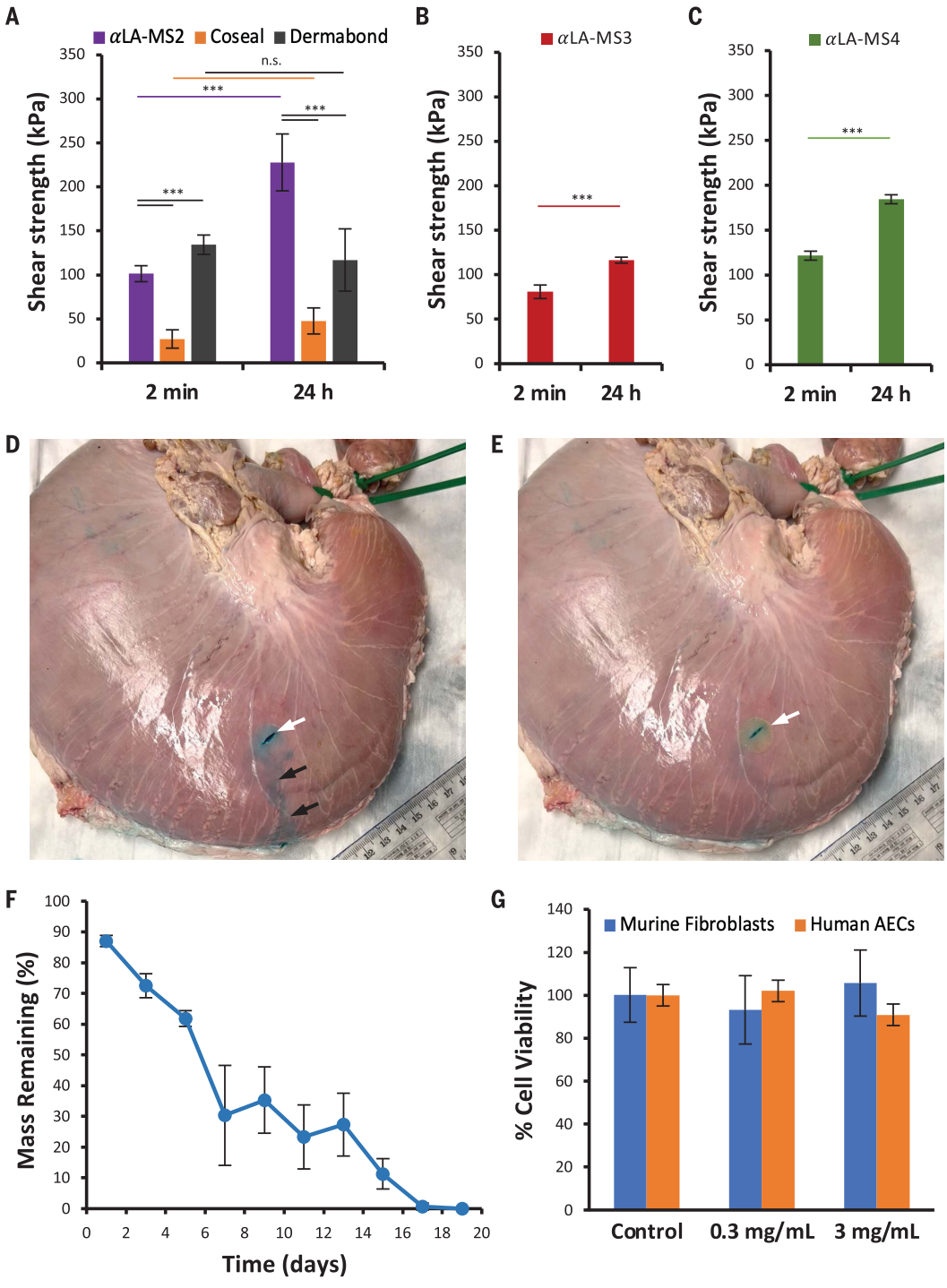

Fig. 3. Ex vivo and in vitro characterization of αLA superglue. (**A**) Lap shear strength comparison of αLA-MS2, Dermabond Advance and CoSeal on wet bovine pericardium. Data are represented as mean ± SD (*N* = 5, except Coseal where *N* = 4). (**B**) Lap shear strength of αLA-MS3 on wet bovine pericardium. Data are represented as mean ± SD (*N* = 5). (**C**) Lap shear strength of αLA-MS4 + αLA-MS2 combination on wet bovine pericardium. Data are represented as mean ± SD (*N* = 5). (**D** and **E**) Ex vivo sealing of perforated porcine stomach using a 15-mm-diameter patch. (D) Picture of a pressurized porcine stomach with an unrepaired 5-mm perforation (white arrow) from which leakage of dyed PBS was observed (black arrows). (E) Picture of a pressurized porcine stomach with a 5-mm perforation, after repair with patch+spray αLA-MS4 + αLA-MS2. No leakage of dyed PBS was observed. (**F** and **G**) In vitro characterization of αLA superglue. (F) In vitro degradation of αLA-MS5. Data are represented as mean ± SD (*N* = 3). (G) Twenty-four-hour viability of murine fibroblasts (NIH 3T3) and human amniotic endothelial cells (AECs) in the presence of αLA-MS2. Data are represented as mean ± SD (*N* = 3). *P* value was calculated with Student's *t* test in Microsoft Excel (2 array, 2 tails, 2 type). n.s., $P > 0.05$; ***$P \leq 0.01$. *N* is the number of independent repetitions.

polymerized monomers followed by compression molding of the solid polymer.

Ex vivo and in vitro testing of αLA superglue

To investigate the tissue adhesive performance, we either sprayed (αLA-MS1 or αLA-MS2), brushed (αLA-MS3), or pressed (αLA-MS4 or αLA-MS5) adhesive onto wet bovine pericardium, formed a lap joint with a second piece of tissue, and incubated the samples in PBS at 37°C. The lap shear strength of the spray formulation αLA-MS2 after 2 min on wet bovine pericardium tissue was 101 ± 9 kPa, which was comparable to Dermabond (134 ± 10 kPa), a medical-grade superglue approved for use in external wound closure (Fig. 3A). The shear strength increased more than twofold to 227 ± 32 kPa after incubation for 24 hours, outperforming Dermabond (116 ± 35 kPa). αLA-MS2 also outperformed the approved polymer hydrogel surgical sealant CoSeal at both the 2-min and 24-hour time points (27 ± 10 kPa; 47 ± 14 kPa) (Fig. 3A). Failure mode analyses of the lap joints indicated cohesive failure both at 2-min and 24-hour incubation, suggesting strong adhesion at the tissue-adhesive interface (fig. S10).

Brush and patch formulations (αLA-MS3 and αLA-MS4, Table 1) were also shown to be effective tissue adhesives (Fig. 3, B and C), as were hybrid formulations in which a patch was augmented with either spray or brush liquids. Ex vivo sealing experiments were

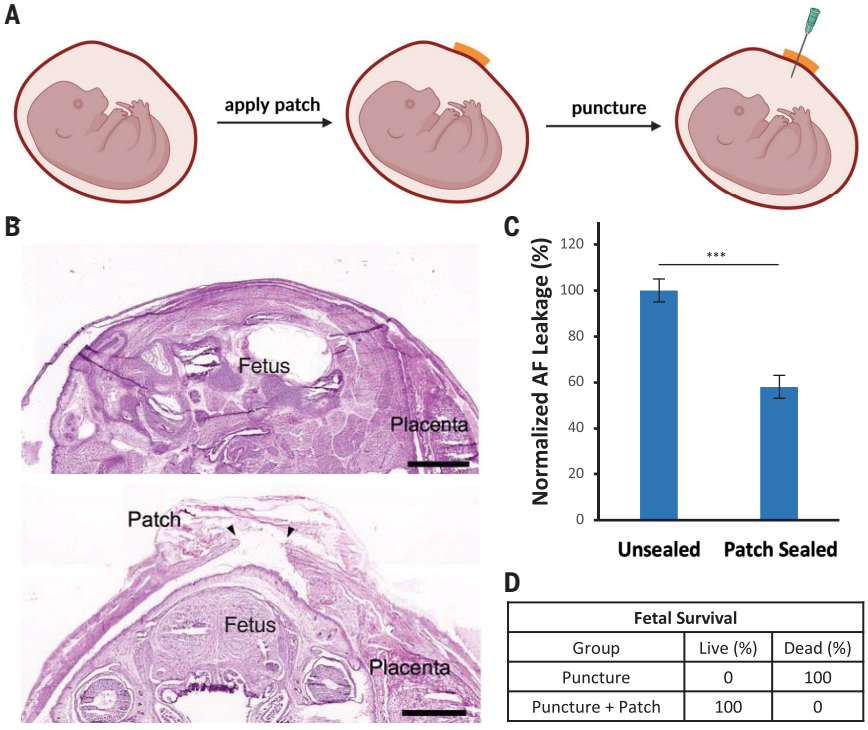

Fetal Survival		
Group	Live (%)	Dead (%)
Puncture	0	100
Puncture + Patch	100	0

Fig. 4. In vivo biological performance of αLA superglue as a fetal membrane sealant. (**A**) Schematic illustration of the model, involving placement of a αLA-MS5 patch followed by puncture through the patch and gestational sac. [Created with BioRender.com]. (**B**) Representative hematoxylin and eosin (H&E)–stained histological images of the gestational sac, placenta, and fetus. The top image shows the native maternal-fetal anatomy prior to puncture at gestation day 15, whereas the bottom image shows a αLA-MS5 + αLA-MS3 presealed and punctured gestational sac at gestation day 18. The patch is well adhered to the myometrium, and the arrowheads indicate the puncture site. Notably, the puncture site is not visible in the patch, suggesting self-healing of the patch following puncture. Scale bar, 1 mm. (**C**) In vivo amniotic fluid leakage after puncture of control (unsealed) and αLA-MS5 + αLA-MS2 presealed gestational sacs. Data are represented as mean ± SD data (N = 7). P value was calculated with Student's t test in Microsoft Excel (2 array, 2 tails, 2 type). ***$P \leq 0.01$. (**D**) Comparison of fetal survival at gestation day 18 for the puncture-only and αLA-MS5 + αLA-MS3 patch presealed groups (N = 5). N is the number of independent repetitions.

performed on fresh porcine stomach, where αLA-MS were effective at stopping leakage from a 5-mm incision despite considerable internal hydrodynamic pressure (Fig. 3, D and E, and movies S3 to S7). Adhesive performance testing of additional formulations on different tissues and substrates (fig. S11), ex vivo sealing of lung (fig. S12), burst strength (fig. S13), swelling (fig. S14), and mechanical repair of a freshly harvested severed bovine tendon (fig. S15) further show the effective and versatile adhesive performance of αLA-MS compared to current surgical sealants and gold standard medical cyanoacrylates (*27*, *29*). Finally, omission of NHS ester significantly diminished lap shear strength (fig. S11), further establishing the importance of NHS ester in αLA polymerization and stabilization of the resulting polymer.

In vitro biological characterization of degradation, cytotoxicity, acute inflammatory response (fig. S16), and bacterial attachment and barrier properties (figs. S17 and S18) were performed. In -vitro degradation of stabilized αLA polymer showed gradual degradation of the polymer over the course of 3 weeks (Fig. 3F), likely due to chain end–mediated depolymerization of αLA polymer (*36*) to yield αLA monomers that pose low risk of toxicity. To evaluate the potential cytotoxicity of the degraded and intact αLA polymer adhesive, we performed cell viability assays using NIH 3T3 mouse fibroblast cells and primary human amniotic epithelial cells. After 24 hours of exposure to αLA polymer, no differences in cell death were observed compared to growth media controls (Fig. 3G and fig. S16). Murine macrophages exposed to αLA polymer resulted in suppression of reactive oxygen species and mRNA expression of the inflammatory cytokine tumor necrosis factor–α (TNF-α) compared to non-treated controls, indicating potential anti-inflammatory properties of the adhesive (fig. S16) (*23*, *34*). Moreover, αLA-MS4 patch and αLA-MS2 spray formulations show resistance to *Escherichia coli* adhesion and penetration, which are important characteristics of medical superglues (figs. S17 and S18) (*24*, *30*, *37*).

In vivo repair of fetal membrane punctures

There is a growing interest in treating a variety of fetal anomalies in utero (*38*). Fetal surgical interventions require breaching of the fetal membranes, which are known to be mechanically fragile and nonhealing (*38*). A major complication of fetal surgery is premature rupture of the membranes (PROM), which occurs in up to 30% of fetal surgery cases and is associated with increased risk of fetal morbidity and mortality, particularly early in gestation (*39*). Biomaterial sealants have been suggested as a means to provide mechanical stability, reduce the loss of amniotic fluid at the surgically created fetal membrane defect, and extend gestation (*40*, *41*). The concept of presealing the fetal membrane with an adhesive prior to intervention has been proposed (*42*), although to our knowledge this strategy has not been tested in vivo.

In an initial trial in timed-pregnant mice at gestational day 15, αLA patches were adhered to the intact myometrium of the gestational sacs in one horn with the aid of a small amount of αLA liquid (Fig. 4A and movie S8). All patches were found intact at gestational day 18, with 100% fetal survival and similar growth in comparison to fetuses in the untreated horn (fig. S19). Histological and immunofluorescence analysis of tissues showed no signs of inflammation or foreign body reaction (figs. S19 and S20), thereby demonstrating that αLA superglue is well tolerated. Upon puncture with a 14-gauge needle (2.1 mm diameter), amniotic fluid loss from presealed membranes was nearly 50% lower compared to unsealed gestational sacs (Fig. 4C, Fig. S21).

We then conducted a comparison of fetal survival following puncture of presealed and unsealed gestational sacs at gestational day 15. In the unsealed and punctured group, 0% fetal survival at gestational day 18 was observed, whereas 100% fetal survival was observed in the presealed and punctured group (Fig. 4D and fig. S22). In the presealed group, fetal growth was normal and the patches remained well adhered to the tissue. The puncture site of the tissue was visible underneath the patch (Fig. 4B), indicating lack of spontaneous healing of the tissue defect. The puncture site was not visible within the patch, which we interpret as being a result of αLA polymer self-healing (Fig. 2D and fig S42).

Stabilized αLA polymer as a pressure-sensitive adhesive

Pressure-sensitive adhesives (PSAs) are commonly used in consumer and industrial products (adhesive tapes, sticky notes, product labels, etc.), where adhesion is typically achieved through the use of viscoelastic polymers with

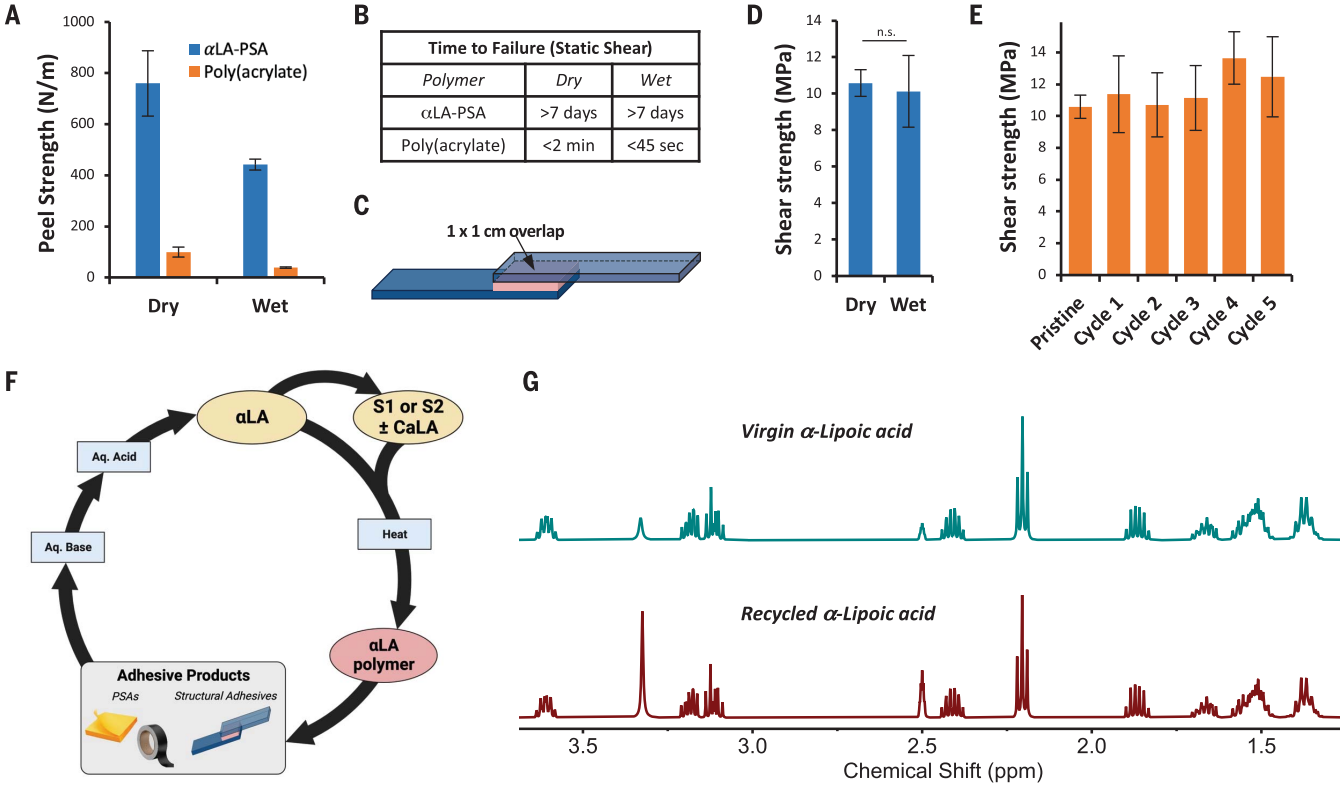

Fig. 5. Pressure-sensitive and structural adhesive performance, and life cycle diagram of stabilized αLA adhesives. (**A** and **B**) Pressure-sensitive adhesion. Peel strength (A) and time to failure under static shear (B) were measured for αLA-PSA against a stainless-steel substrate, in dry and wet conditions. For wet performance, the PSA and substrate were fully submerged in water before making contact. Data are represented as mean ± SD [peel strength N = 5, except for poly(acrylate) where N = 4; time to failure N = 3]. (**C** to **E**) Structural adhesive performance of αLA-SA (containing αLA, CaLA, and S2) under dry and wet conditions. (C) Aluminum bars were bonded together with αLA-SA to make a lap shear joint with a 1-cm^2 overlap. (D) Lap shear bond strength of structural adhesive αLA-SA (containing αLA, CaLA, and S2) under dry and wet conditions. Wet samples were assembled and bonded in air and then immersed in water for 24 hours before testing. Data are represented as mean ± SD (N = 5). P value was calculated with Student's t test in Microsoft Excel (2 array, 2 tails, 2 type). n.s., P > 0.05. (E) Strong adhesive bonds could be regenerated by reassembling ruptured surfaces and heating to 100°C for 10 min. No evidence of strength attenuation was observed over multiple cycles. Data are represented as mean ± SD (N = 5). (**F**) Closed-loop life cycle diagram of stabilized αLA PSA and structural adhesives. Virgin αLA monomer, in combination with stabilizer S1 or S2 (structural adhesives also contain CaLA), are thermally polymerized to yield stabilized αLA polymer, which is then processed into a PSA or structural adhesive product. After service, a two-step aqueous extraction regenerates αLA monomer feedstock, which can then reenter the cycle. [Created with BioRender.com] (**G**). Comparison ^{1}H NMR spectra showing that virgin versus recycled αLA are chemically identical. DMSO-d6, 2.5 parts per million (ppm); water, 3.3 ppm. N is the number of independent repetitions.

low T_g (*1*). Polymers of αLA would seem to be excellent PSA candidates by virtue of their subambient T_g values (*22*, *43*); however, depolymerization of unstabilized αLA polymers represents a large obstacle to practical use. To illustrate this, a thin thermally polymerized film of αLA polymer on PET backing that was initially sticky to the touch became nonfunctional as a PSA within 2 to 3 days as a consequence of depolymerization and the gradual formation of crystalline αLA domains (fig. S23).

Stabilized αLA polymers offer a potential solution to this challenge. To illustrate this, a stabilized αLA polymer PSA (αLA-PSA) was prepared as a thin coating on PET backing as described above but with the addition of S2 monomer. Heating to 100°C resulted in a conformal and stable sticky viscoelastic polymer that retained PSA-like properties for several months under ambient conditions. As shown by 180° peel tests, αLA-PSA exhibited a dry peel strength of 760 ± 127 N/m against stainless steel (SS) (Fig. 5A and figs. S24 and S25), significantly higher than a conventional PSA polymer (99 ± 19 N/m) obtained from butyl acrylate (BA) and acrylic acid (AA) (mole ratio 95:5). For αLA-PSA on PET bonded to SS and high-density polyethylene (HDPE), elapsed time to failure under a static 1-kg load was >7 days, whereas a conventional BA-AA PSA polymer failed in under 2 min under the same conditions (Fig. 5B).

αLA-PSA performance was also tested in water, a challenging condition for conventional PSAs (*44*). Samples were assembled and held under water for 24 hours before measurement. αLA-PSA on PET backing exhibited a wet peel strength of 441 ± 21 N/m against SS, outperforming a conventional PSA polymer that showed a wet peel strength of only 38 ± 2.5 N/m (Fig. 5A and fig. S25). In static shear testing under water, we did not observe failure of αLA-PSA in the first 7 days, whereas conventional polyacrylate PSA failed in less than 45 s (Fig. 5B). Further static shear testing showed that αLA-PSA could support >6 kg of weight when applied to SS and HDPE in water (fig. S24). A sticky note created by coating water-resistant paper with αLA-PSA (contact area of 7.5 cm^2) was capable of sustaining a static 500-g load over 7 days without failure under water (fig. S24). Repeated removal and repositioning of the submerged αLA-PSA sticky note did not affect its performance (movie S9).

Stabilized αLA polymer as a structural adhesive

Designing a αLA polymer adhesive with strength comparable to that of epoxies and other structural adhesives (*1*, *45*–*47*) is inherently challenging owing to the soft and viscoelastic

nature of αLA polymers. We postulated that the addition of a divalent ion salt of αLA (e.g., calcium lipoate, CaLA) would confer strength and rigidity to otherwise soft αLA polymers. Heating a powder admixture of αLA and CaLA revealed a low-temperature monomer melting transition (T_m = 58°C) in both first and second heating cycles, indicating inefficient monomer conversion (or rapid depolymerization) (fig. S26). Stability afforded by the addition of S1 or S2 proved to be the key to obtaining stable and strong structural adhesives. Differential scanning calorimetry analysis of an admixture of αLA, CaLA, and S1 (αLA-SA, Table 1) powders revealed an endothermic monomer melting transition in the first heating cycle, which disappeared in the second heating cycle in favor of a glass transition (T_g −20°C) and broad polymer melt-like transition (135°C), indicating polymerization of the monomer mixture into a cross-linked polymer network in which CaLA acts as a rigidifying cross-linker (fig. S26). The lap shear strength of aluminum bars bonded by αLA-SA cured at 100°C for 10 min was high (10.5 ± 7 MPa) and remained unchanged (10.1 ± 1.9 MPa) even after submerging in water for 24 hours (Fig. 5D and figs. S27 and S36). The measured lap shear strength for αLA-SA is comparable to or greater than reported values for aluminum substrates adhered using unreinforced bisphenol A–based epoxies (*45*–*47*). Ruptured lap shear joints could be easily rejoined by heating at 100°C for 10 min, with no significant reduction in strength over five cycles (Fig. 5E), highlighting a balance of polymer network dynamics, rigidity, and strength. Thus, αLA-SA structural adhesive can be a potential alternative to epoxy thermosets but with advantages that include short curing times, resistance to the deleterious effects of water, and the ability to be reprocessed through mild heating.

Closed-loop recycling of stabilized αLA polymer adhesives

Worldwide production of adhesives was estimated to be 20 million metric tons in 2019 (*48*). Among the largest categories are PSA and structural adhesives, many of which are currently petroleum-derived and nonrecyclable. Despite growing efforts to fabricate adhesives from sustainable source materials, few reports exist of PSAs and structural adhesives that can be recycled into reusable feedstocks (*6*, *7*, *49*). αLA polymers are attractive sustainable adhesive candidates because they are derived from a monomer that can be biomanufactured (*50*), and they can be chemically recycled to monomeric feedstock (*13*) in aqueous solvent. To demonstrate the latter, αLA-PSA on PET tape was immersed in aqueous 0.5M NaOH, followed by removal of the PET backing and acidification of the solution to precipitate solid αLA with 82% yield (Fig. 5F). High-performance liquid chromatography and ^{1}H NMR analysis confirmed the high purity of the recycled αLA (Fig. 5G and figs. S28 and S29). We further showed that stabilized αLA-PSA integrated into multilayer films, such as those found in consumer packaging, could be recycled using the same approach (figs. S30 and S31). The presence of S1, S2, and CaLA in the adhesive formulation did not interfere with monomer recycling, and these comonomers can be synthesized from regenerated αLA.

Conclusions

In this work, we addressed a long-standing challenge to translation of αLA polymers, creating a recyclable adhesive for medical, consumer, and industrial applications. The key enabling discovery was that electrophilically modified αLA (e.g., S1 or S2) accelerates αLA polymerization at room temperature and stabilizes the resulting polymer against depolymerization, thus opening the door to a diverse family of αLA polymer adhesives. In the case of surgical superglue, ultrafast polymerization of αLA induced by contact with wet tissue enables rapid and robust bonding to tissue, with mechanical and biological performance superior to existing medical-grade cyanoacrylate superglue. Within our modular monomer system, fine-tuning the monomer composition allowed the properties to be adapted for use in highly diverse contexts such as pressure-sensitive and structural adhesion. The performance of stabilized αLA polymer PSAs and SAs is competitive with or exceeds that of existing marketed adhesives, while also offering circular economy advantages due to facile closed-loop monomer recycling in aqueous media.

REFERENCES AND NOTES

1. A. V. Pocius, *Adhesion and Adhesives Technology: An Introduction* (Carl Hanser Verlag, 2012).
2. J. Li *et al*., *Science* **357**, 378–381 (2017).
3. D. Hwang *et al*., *Nat. Mater.* **22**, 1030–1038 (2023).
4. Z. Wang, X. Wan, S. Wang, *Chem* **9**, 771–783 (2023).
5. Y. Chen *et al*., *Adv. Funct. Mater.* **30**, 1905287 (2020).
6. D. E. Packham, "15 - The environmental impact of adhesives" in, F. Pacheco-Torgal, L. F. Cabeza, J. Labrincha, A. B. T.-E. C. and B. M. de Magalhães, Eds. (Woodhead Publishing, 2014; 338–367, https://www.sciencedirect.com/science/article/pii/B9780857097675500157).
7. M. Shen, H. Cao, M. L. Robertson, *Annu. Rev. Chem. Biomol. Eng.* **11**, 183–201 (2020).
8. C. R. Westerman, B. C. McGill, J. J. Wilker, *Nature* **621**, 306–311 (2023).
9. Y.-F. Lei *et al*., *ACS Sustain. Chem.& Eng.* **8**, 13261–13270 (2020).
10. M. A. Droesbeke, A. Simula, J. M. Asua, F. E. Du Prez, *Green Chem.* **22**, 4561–4569 (2020).
11. A. Beharaj, E. Z. McCaslin, W. A. Blessing, M. W. Grinstaff, *Nat. Commun.* **10**, 5478 (2019).
12. Q. Zhang *et al*., *Sci. Adv.* **4**, eaat8192 (2018).
13. Q. Zhang *et al*., *Matter* **4**, 1352–1364 (2021).
14. K. V. Dikshit, A. M. Visal, F. Janssen, A. Larsen, C. J. Bruns, *ACS Appl. Mater. Interfaces* **15**, 17256–17267 (2023).
15. R. C. Thomas, L. J. Reed, *J. Am. Chem. Soc.* **78**, 6148–6149 (1956).
16. A. Kisanuki *et al*., *J. Polym. Sci. A Polym. Chem.* **48**, 5247–5253 (2010).
17. Y. Liu, Y. Jia, Q. Wu, J. S. Moore, *J. Am. Chem. Soc.* **141**, 17075–17080 (2019).
18. X. Zhang, R. M. Waymouth, *J. Am. Chem. Soc.* **139**, 3822–3833 (2017).
19. M. A. Alraddadi, V. Chiaradia, C. J. Stubbs, J. C. Worch, A. P. Dove, *Polym. Chem.* **12**, 5796–5802 (2021).
20. B.-S. Wang *et al*., *Angew. Chem. Int. Ed.* **62**, e202215329 (2023).
21. E.-K. Bang *et al*., *J. Am. Chem. Soc.* **135**, 2088–2091 (2013).
22. K. R. Albanese, P. T. Morris, J. Read de Alaniz, C. M. Bates, C. J. Hawker, *J. Am. Chem. Soc.* **145**, 22728–22734 (2023).
23. C. Chen *et al*., *Green Chem.* **23**, 1794–1804 (2021).
24. J. Chen, T. Yuan, Z. Liu, *Biomater. Sci.* **8**, 6235–6245 (2020).
25. J. Houk, G. M. Whitesides, *J. Am. Chem. Soc.* **109**, 6825–6836 (1987).
26. S. Aoshima, S. Kanaoka, *Chem. Rev.* **109**, 5245–5287 (2009).
27. S. Nam, D. Mooney, *Chem. Rev.* **121**, 11336–11384 (2021).
28. G. M. Taboada *et al*., *Nat. Rev. Mater.* **5**, 310–329 (2020).
29. V. Bhagat, M. L. Becker, *Biomacromolecules* **18**, 3009–3039 (2017).
30. E. Petrie, *Rev. Adhes. Adhes.* **2**, 253–310 (2014).
31. A. J. Singer, J. V. Quinn, J. E. Hollander, *Am. J. Emerg. Med.* **26**, 490–496 (2008).
32. D. H. Park *et al*., *J. Appl. Polym. Sci.* **89**, 3272–3278 (2003).
33. X. Ke *et al*., *ACS Appl. Mater. Interfaces* **14**, 53546–53557 (2022).
34. C. Liu *et al*., *Chem. Mater.* **35**, 2588–2599 (2023).
35. C. Cui *et al*., *Nat. Commun.* **14**, 7707 (2023).
36. J. Guo, S. Zhang, Y. Tao, B. Fan, W. Tang, *Polym. Chem.* **13**, 6637–6649 (2022).
37. U. Narang, L. Mainwaring, G. Spath, J. Barefoot, *J. Cutan. Med. Surg.* **7**, 13–19 (2003).
38. J. A. Deprest *et al*., *Prenat. Diagn.* **30**, 653–667 (2010).
39. R. Devlieger, L. K. Millar, G. Bryant-Greenwood, L. Lewi, J. A. Deprest, *Am. J. Obstet. Gynecol.* **195**, 1512–1520 (2006).
40. S. M. Winkler, M. R. Harrison, P. B. Messersmith, *Biomater. Sci.* **7**, 3092–3109 (2019).
41. E. Avilla-Royo, N. Ochsenbein-Kölble, L. Vonzun, M. Ehrbar, *Biomater. Sci.* **10**, 3695–3715 (2022).
42. H. K. Carnaghan, M. R. Harrison, *Eur. J. Obstet. Gynecol. Reprod. Biol.* **144** (suppl. 1), S142–S145 (2009).
43. J. Li *et al*., *Adv. Mater. Interfaces* **10**, 2202005 (2023).
44. B. D. B. Tiu, P. Delparastan, M. R. Ney, M. Gerst, P. B. Messersmith, *ACS Appl. Mater. Interfaces* **11**, 28296–28306 (2019).
45. D. A. Dillard, Ed., *Advances in Structural Adhesive Bonding* (Woodhead, 2010).
46. R. Moriche *et al*., *Int. J. Adhes. Adhes.* **68**, 407–410 (2016).
47. M. Mansourian-Tabaei, S. H. Jafari, H. A. Khonakdar, *J. Appl. Polym. Sci.* **131**, app.40017 (2014).
48. Adhesives and Sealants Industry, (2016), https://www.adhesivesmag.com/articles/94543-construction-growth-driving-adhesive-and-sealant-demand.
49. K. L. Law, R. Narayan, *Nat. Rev. Mater.* **7**, 104–116 (2022).
50. D. Lennox-Hvenekilde *et al*., *Metab. Eng.* **76**, 39–49 (2023).

ACKNOWLEDGMENTS

We thank E. Carvalho, a member of Kumar laboratories at the University of California, Berkeley, for providing access and assistance with the rheometer. We acknowledge the NMR facility at the College of Chemistry NMR facility at the University of California, Berkeley. **Funding:** We thank the Life Sciences Entrepreneurship Center at UC Berkeley for partial support. S.P. thanks the Swiss National Science Foundation (SNSF) postdoc mobility fellowship P500PN_202898 for providing support. K.D. thanks National Science Foundation Graduate Research Fellowship under grant no. DGE 1752814. M.A. thanks Scientific and Technological Research Council of Turkey (TUBITAK, BIDEB-2219 International Postdoctoral Research Scholarship Program). **Author contributions:** S.P. and P.B.M. designed the project. S.P. developed the reaction conditions and synthesized the reagents. S.P., K.D., and H.C. performed all polymerization and adhesion analyses. S.P. and K.D. performed ex vivo experiments. K.D. performed in vitro studies. J.S. conducted antibacterial and in vivo studies. S.P., M.A., and D.R. performed the adhesion studies of the structural adhesive. S.P. and P.B.M. wrote the manuscript, and all authors reviewed the manuscript. **Competing interests:** S.P., K.D., J.S., and P.B.M. filed a PCT/US24/24635 patent as co-inventors. S.P., K.D., J.S., and P.B.M. have a financial interest in AsparaGlue Inc., a company that is commercializing this technology. **Data and materials availability:** All data are available in the main text or the supplementary materials.

SUPPLEMENTARY MATERIALS

science.org/doi/10.1126/science.ado6292
Materials and Methods
Figs. S1 to S42
Table S1
Reference (*51*)
MDAR Reproducibility Checklist
Movies S1 to S9

Submitted 12 February 2024; accepted 26 June 2024
10.1126/science.ado6292